Available online at www.sciencedirect.com
SCIENCE DIRECT®
Physics of the Earth and Planetary Interiors 143–144 (2004) 507–514
PHYSICS OF THE EARTH AND PLANETARY INTERIORS
www.elsevier.com/locate/pepi

A new large-volume multianvil system

D.J. Frost [a,*], B.T. Poe [a,b], R.G. Trønnes [c], C. Liebske [a], A. Duba [a,d], D.C. Rubie [a]

[a] *Bayerisches Geoinstitut, Universität Bayreuth, D-95440 Bayreuth, Germany*
[b] *Dipartimento di Scienze della Terra, Università degli Studi "G. D'Annunzio"-Chieti, 66013 Chieti Scalo, Italy*
[c] *Nordic Volcanological Institute, Grensásvegur 50, IS-108 Reykjavík, Iceland*
[d] *American Museum of Natural History, Central Park West at 79th St., NYC, New York 10024, USA*

Abstract

A scaled-up version of the 6–8 Kwai-type multianvil apparatus has been developed at the Bayerisches Geoinstitut for operation over ranges of pressure and temperature attainable in conventional systems but with much larger sample volumes. This split-cylinder multianvil system is used with a hydraulic press that can generate loads of up to 5000 t (50 MN). The six tool-steel outer-anvils define a cubic cavity of 100 mm edge-length in which eight 54 mm tungsten carbide cubic inner-anvils are compressed. Experiments are performed using Cr_2O_3-doped MgO octahedra and pyrophyllite gaskets. Pressure calibrations at room temperature and high temperature have been performed with 14/8, 18/8, 18/11, 25/17 and 25/15 OEL/TEL (octahedral edge-length/anvil truncation edge-length, in millimetre) configurations. All configurations tested reach a limiting plateau where the sample-pressure no longer increases with applied load. Calibrations with different configurations show that greater sample-pressure efficiency can be achieved by increasing the OEL/TEL ratio. With the 18/8 configuration the GaP transition is reached at a load of 2500 t whereas using the 14/8 assembly this pressure cannot be reached even at substantially higher loads. With an applied load of 2000 t the 18/8 can produce $MgSiO_3$ perovskite at 1900 °C with a sample volume of ~20 mm^3, compared with <3 mm^3 in conventional multianvil systems at the same conditions. The large octahedron size and use of a stepped $LaCrO_3$ heater also results in significantly lower thermal gradients over the sample.

Keywords: Multianvil; Large-volume; High pressure; Pressure calibration

1. Introduction

Multianvil devices in a number of different configurations have been used for many years to generate pressures in the range 3–28 GPa while simultaneously heating to temperatures up to 3000 K. The pressure range can be extended to over 50 GPa using inner-anvils of sintered diamond (Ito, Kubo, and Funakoshi personal communication). The 6–8 type multianvil system (Kawai and Endo, 1970; Kawai et al., 1973; Ohtani et al., 1987; Walker et al., 1990) has been particularly successful due to its ability to apply stable high pressures and temperatures for significant periods of time (up to several weeks in some cases) with sample volumes large enough to be analysed using a range of conventional characterization methods. This system employs six tool-steel outer-anvils and eight tungsten carbide cubic inner-anvils to focus an applied load on an octahedral high-pressure chamber formed as a result of corner truncations on the inner-anvils. The anvils are compressed using a hydraulic press often with a 1000–2000 t (10–20 MN) capacity. By varying the corner truncation size of the inner-anvils, various sample-pressure ranges can be attained. Using

* Corresponding author. Tel.: +49-921-553737; fax: +49-921-553769.
E-mail address: dan.frost@uni-bayreuth.de (D.J. Frost).

0031-9201/$ – see front matter © 2004 Elsevier B.V. All rights reserved.
doi:10.1016/j.pepi.2004.03.003

press loads of approximately 900 t, for example, and inner-anvil truncations of 3 mm it is possible to reach sample-pressures of approximately 26 GPa. With such small inner-anvil truncations, however, the sample volume at these conditions is small, (on the order of 2 mm^3 or less), and accurate control over the temperature environment is difficult due to high thermal gradients. A number of modern analysis techniques such as NMR, calorimetry and neutron diffraction require much larger sample yields. In addition, many in situ techniques require large assembly volumes for precise measurements, for the incorporation of multiple thermocouples and in order to establish well-controlled thermal environments (e.g. Xu et al., 2004).

Here we describe a scaled-up version of the 6–8 multianvil system, which has been designed with the aim of providing significantly larger sample volumes than those of conventional systems while still operating over a similar pressure and temperature range. A particular aim of the system is to reach pressures compatible with the lower mantle and to facilitate the synthesis of (Mg, Fe)SiO_3 perovskite, the dominant phase in Earth's lower mantle, with sample volumes in excess of 10 mm^3. Extrapolation of existing calibration curves suggests that loads on the order of 3000–4000 t may be necessary to produce pressures in excess of 20 GPa with such sample volumes and for this reason the system was designed for use with a 5000 t hydraulic press.

In addition to describing the dimensions of the device and the materials employed in construction of the guide blocks and anvils, we also discuss the development and calibration of high-pressure assemblies and describe briefly some experimental applications.

2. Experimental description

In the large-volume multianvil system two "guide blocks", with dimensions that have been scaled-up in comparison to conventional systems, are compressed using a 5000 t (50 MN) hydraulic press. Each guide block consists of three tool-steel outer-anvils separated by three smaller support wedges (Fig. 1) inside a 1.2 m × 1.2 m × 0.196 m steel platen. A finite-element calculation showed that using three separate support wedges, as shown in Fig. 1, significantly reduces the tensile stresses in the surrounding outer platen. After initial testing, additional 40 mm thick tool-steel load distribution disks were included below each guide

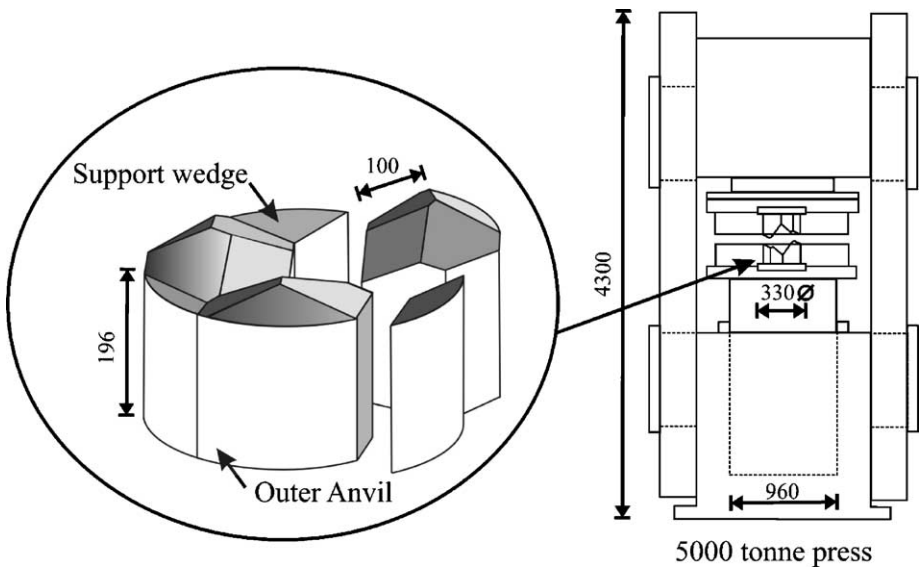

Fig. 1. Schematic diagram of the six wedges of the guide block. The three outer-anvils are separated along the outer circumference by three support wedges (see text for details). The inset to the right shows the 5000 t (50 MN) press frame with the two guide blocks inside steel platens on top of the 960 mm diameter ram. All dimensions are in millimetre.

Table 1

Assembly	Capsule size		Gaskets		Estimated P_{max} (GPa)	Load at P_{max} (T)
OEL/TEL (mm)	Ø (mm)	Length (mm)	Thickness (mm)	Width (mm)		
25/17	5	4	3.7	6.0	13	3000
25/15	4	4	4.7	6.0	16	2500
18/11	2	3.5	3.0	5.0	19	2000
18/8	2	3.5	4.7	5.0	23	2500
14/8	1.5	2.5	2.5	5.0	21	2000

block. The three main outer-anvils define an inner cubic cavity of 100 mm edge-length in which the eight second-stage tungsten carbide inner-anvils are compressed. The large inner cubic cavity dimension enables forces up to 5000 t (50 MN) to be applied while ensuring that stresses at this interface lie well below the strength of the outer-anvils. Toshiba "F" grade tungsten carbide second-stage anvils are used, each with an edge-length of 54 mm. The dimensions of the inner-anvil truncations, octahedral assemblies and pyrophyllite gaskets employed are given in Table 1. Due to the combined weight of the eight second-stage anvils (18.5 kg) the cubes are assembled inside the lower guide block. Balsa-wood spacers are used between the cubes to provide initial alignment of the anvils. Epoxy-impregnated fibreglass laminate sheets 105 mm × 105 mm × 0.8 mm are used to electrically insulate the inner-anvils from the guide blocks. Cardboard and Teflon tape are placed on the surface of the cubes behind the gaskets to electrically insulate the thermocouple wires and to provide extra support to the gaskets.

The octahedral pressure assemblies used in the large-volume system are similar to those described elsewhere (Liebermann and Wang, 1992; Walter et al., 1995; Rubie, 1999). Some modifications, similar to those made on a piston cylinder assembly by Wade and Wood (2002), have been made, however, in order to develop an assembly that can reach temperatures >2400 °C. A diagram of this assembly is shown in Fig. 2. In order to avoid reaction or eutectic melting between various ceramic materials at high temperature, the $LaCrO_3$ furnace is completely surrounded by MgO and the thermocouple sleeve, which is normally Al_2O_3, is also made from MgO. A thin ZrO_2 sleeve for thermal insulation is inserted around the furnace, but is separated from it by an MgO sleeve. A single crystal MgO sample capsule is employed, which is particularly effective in keeping metallic liquids enclosed due to the absence of wettable grain boundaries. Ultramafic silicate liquids can also be contained for short periods of time at high pressures and temperatures because such liquids are close to being in chemical equilibrium with MgO. The resulting

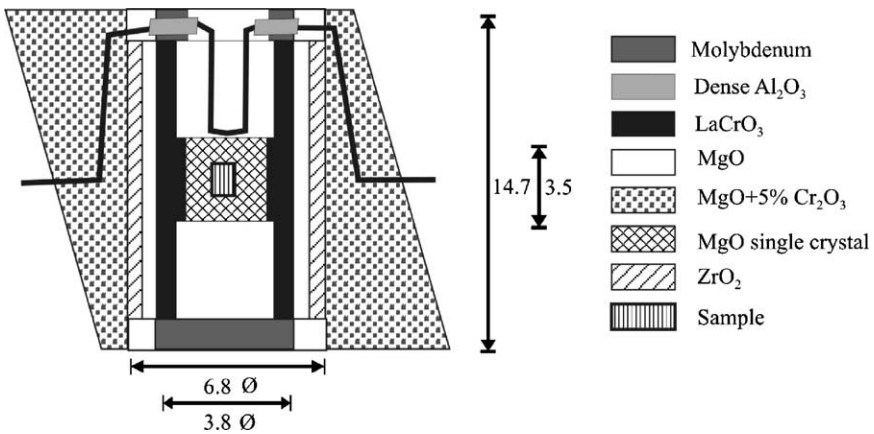

Fig. 2. Cross-section through the 18/8 assembly, modified for high temperatures. All assemblies used in the press follow a similar design.

assembly is less power-efficient than when a single thick ZrO_2 sleeve is used around the furnace, but can be heated stably to much higher temperatures (~2800 °C).

3. Calibration

Calibrations have been performed using 25/17, 25/15, 18/11, 18/8 and 14/8 (octahedral edge-length/truncation edge-length, in millimetre) assemblies. Room temperature calibrations were performed using the Bi I–II and III–V transitions at 2.52 ± 0.05 GPa and 7.7 Gpa, respectively (Getting, 1998; Lloyd, 1971), ZnS at 15.5 ± 0.7 GPa, GaAs at 18.8 ± 0.8 GPa (Onodera and Ohtani, 1980) and GaP at 22.5 GPa (Dunn and Bundy, 1978). At high temperature the transformations of $CaGeO_3$ garnet to perovskite (Susaki et al., 1985), SiO_2 coesite to stishovite (Zhang et al., 1996), Mg_2SiO_4 forsterite to wadsleyite (Morishima et al., 1994), wadsleyite to ringwoodite (Suzuki et al., 2000) and $MgSiO_3$ majorite to perovskite (Fei et al., 1990) were bracketed in a series of quench experiments. The high temperature calibrations were performed using mixtures of both high- and low-pressure phases in the starting material.

4. Results

Room temperature calibrations for five assemblies are shown in Fig. 3. For all assemblies, the pressure reaches a plateau where the application of considerably higher loads does not produce a significant increase in the sample-pressure. This can be seen most clearly in the 18/8 calibration, where a doubling of the applied load is required to raise the pressure by 4.2 GPa from the GaAs to the GaP transition. This severe reduction in pressure efficiency defines the useful high-pressure limit of the assembly (P_{max} in Table 1). This limit is also clearly indicated by the transitions that cannot be attained using the assemblies up to 3500 t. The ZnS (15.5 GPa) transition in the 25/17, the GaAs transition in the 25/15 and the GaP transformation in the 14/8 or 18/11 are not observed with the application of loads up to 3500 t.

High-temperature pressure calibrations are shown in Fig. 4. For each assembly a higher efficiency in

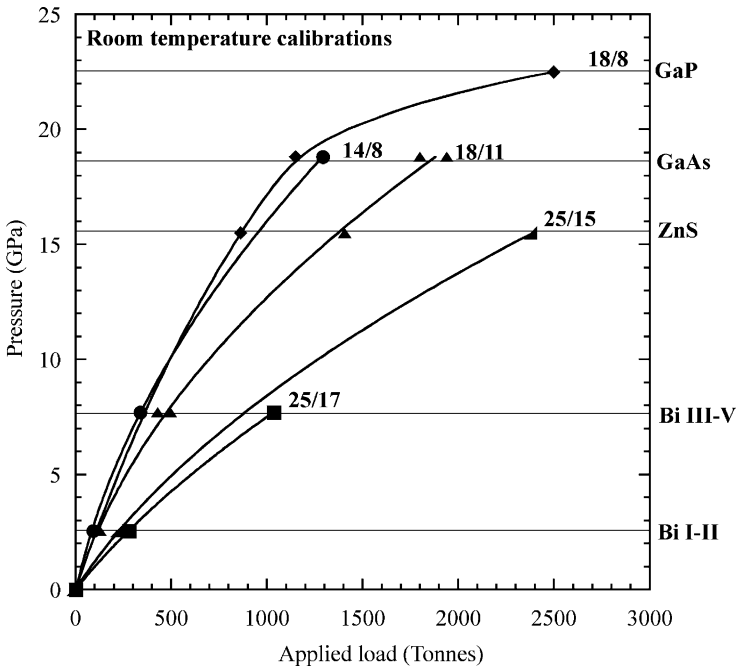

Fig. 3. Pressure calibration curves obtained at room temperature. See text for details on pressure uncertainties.

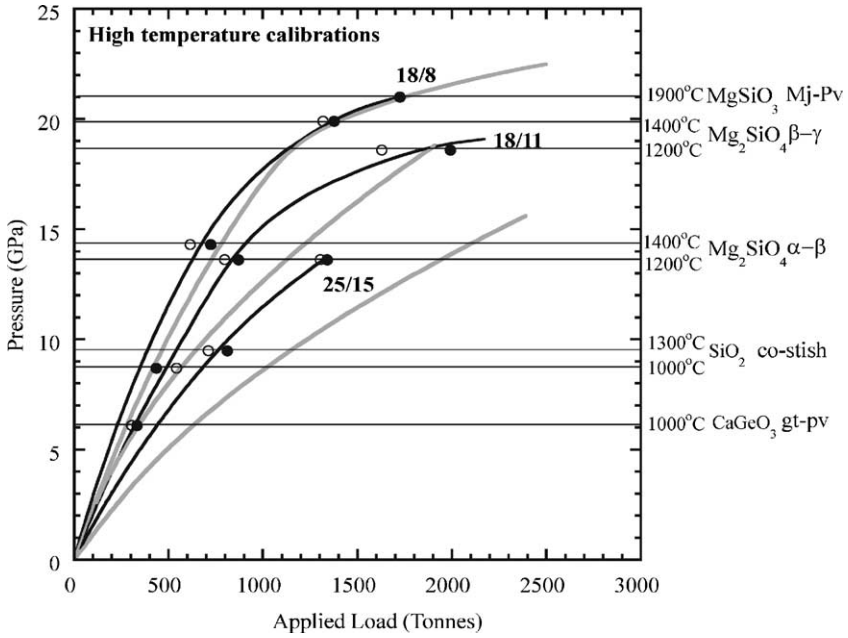

Fig. 4. High-temperature pressure calibration curves are shown (black lines). Room temperature calibrations (grey) plot below the high temperature curves of each assembly. The transformations on which the calibrations are based are $CaGeO_3$ garnet to perovskite (gt–pv), SiO_2 coesite to stishovite (co–stish), Mg_2SiO_4 forsterite to wadsleyite (α–β) and wadsleyite to ringwoodite (β–γ), and $MgSiO_3$ majorite to perovskite (Mj–Pv). The occurrence of either the high or low-pressure phase at each transformation is indicated by either filled or opened circles respectively.

generating pressure is observed at high temperature compared with room temperature but the difference between the high- and low-temperature calibration curves decreases as the size of the assembly decreases. For the 18/8, the high- and low-temperature curves are almost identical. Although there is a considerable reduction in the efficiency of pressure generation when using the 18/8 assembly above 18 GPa, samples of pure $MgSiO_3$ perovskite can be synthesized from enstatite starting materials in this assembly between 1800 and 1900 °C and with applied loads of 2000 t.

Uncertainties in the absolute pressures of room temperature and high temperature transformations, particularly at pressures above 10 GPa, are difficult to assess but are most likely at least 1 GPa. A range of determined pressures can be found in the literature for each room temperature fixed point transition above 10 GPa (see Onodera and Ohtani, 1980). This range probably arises from differences in pressure calibrant employed and due to varying states of non-hydrostatic stress. Similarly, calibrations of high temperature transformations have uncertainties associated with the bracketing of the reaction and the pressure calibrant employed. However, because we are mainly interested in the differences in pressure efficiency between the different assemblies and we have tried to use similar transformations for all assemblies, large absolute pressure uncertainties will not significantly affect our conclusions.

5. Discussion

The plateau in pressure generation that occurs for all assemblies at high loads results in an effective upper limit in the attainable sample-pressure (P_{max} in Table 1). Based on Fig. 4, for example, the 18/11 assembly is unlikely to produce sample-pressures that significantly exceed 20 GPa, no matter how large a press is employed. This plateau is most likely related to the gasketing. Each incremental increase in pressure must be associated with a decrease in volume of the assembly and a decrease in thickness of the

gaskets. The plateau most likely occurs at loads where both extrusion and compressibility of the gaskets are significantly reduced and a large proportion of the additional load becomes supported by the gaskets. It has previously been recognised that pyrophyllite may not be the optimal gasket material for multianvil devices at pressures above 10 GPa (Yoneda et al., 1984) and that composite gaskets may be more suitable. An interesting feature of the room-temperature calibrations, however, is that the 18/8 assembly is more pressure efficient than the 14/8 assembly, even though the anvil truncations are the same and the volume of the 18 mm assembly after the experiment is larger. The increased efficiency of the 18/8 assembly may be a result of the larger amount of MgO from the octahedral assembly that becomes extruded into the gasket in comparison with the 14/8. In all assemblies some MgO is extruded into the gasket but the amount of MgO extrusion will increase with increasing OEL/TEL. A composite gasket is formed during compression with stiffer MgO in the higher-pressure region and softer pyrophyllite at the lower pressure side. Both 14/8 and 18/8 gaskets have a similar width after an experiment (∼13 mm) but the increased amount of stronger MgO in the 18/8 gaskets probably results in a steeper pressure gradient across the gasket and therefore a smaller loss of load into the gasket region. This small increase in pressure efficiency makes a crucial difference because, in comparison with the 18/8, the 14/8 assembly cannot reach the GaP transformation at room temperature or the $MgSiO_3$ perovskite stability field at high temperature.

The survival rate of the tungsten carbide inner-anvils is very good, with anvils only very occasionally being damaged after experiments at more extreme conditions e.g. 18/8 experiments with long heating times (>5 h) at high temperatures (>2000 °C) and pressures (>20 GPa). Blow-outs, (i.e. instantaneous losses in pressure usually resulting in the fracture of tungsten carbide anvils), are rare and occur almost exclusively during compression with anvils which were most likely internally damaged during a previous experiment at the extreme conditions described above. In initial experiments using the 25/15 assembly several anvils were fractured after each experiment. This problem was alleviated, however, by replacing the alumina 4-bore thermocouple tubing with similar tubing of MgO. The relatively incompressible alumina thermocouple tube most likely caused higher stresses to accumulate in the axial direction of the assembly.

Temperature calibrations for the 18/8 and 18/11 assemblies using enstatite-diopside pyroxene thermometry at 1300 °C show that axial thermal gradients are approximately 50 °C/mm along the length of the capsules. The thermal gradients in 10/5 and 10/4 assemblies using conventional 32 mm anvil systems at similar pressures are about 100 °C/mm (Canil, 1994; Walter et al., 1995). Fig. 5 shows a multiple Re capsule in which five sample chambers contained Mg_2SiO_4 samples that were melted at 18 GPa and 2250 °C in an 18/11 assembly. In each chamber an identical phase assemblage of approximately 10% MgO crystals in equilibrium with melt was produced. The consistency in the proportion of MgO in each capsule indicates that the radial thermal gradients were less than 20°/mm, even at these relatively high temperatures. Using this type of multi-capsule, a range of different compositions can be melted in the same experiment such that relative melting temperatures can be accurately determined.

The use of larger assemblies at high pressures facilitates synthesis experiments in which large sample volumes are essential for subsequent characterization at ambient conditions (for example, using NMR—see Kohn et al., 2002). Large sample volumes are also essential for many physical property measurements, such as thermal diffusivity, electrical conductivity and elastic properties using ultrasonic measurements (e.g. Xu et al., 2004). In addition, such in-situ measurements often require the use of more than one thermocouple, which is also facilitated by using a large sample assembly. Thermal diffusivity measurements, for example, require both a large sample volume and the insertion of two thermocouples. One thermocouple on the outside surface of the sample is used to control and fluctuate the temperature in a sinusoidal manner, while a second thermocouple in the centre of the sample records the time lag in the temperature curve that results from thermal diffusion. Using Angstrom's method (Khedari et al., 1995), the thermal diffusivity can be determined from analysis of this time lag in relation to the distance between the thermocouples, which is also more accurately established in larger assemblies. Such measurements have been made on wadsleyite and ringwoodite in the large-volume press up to 20 GPa and 1100 °C (Xu et al., 2004). For ultrasonic measurements the

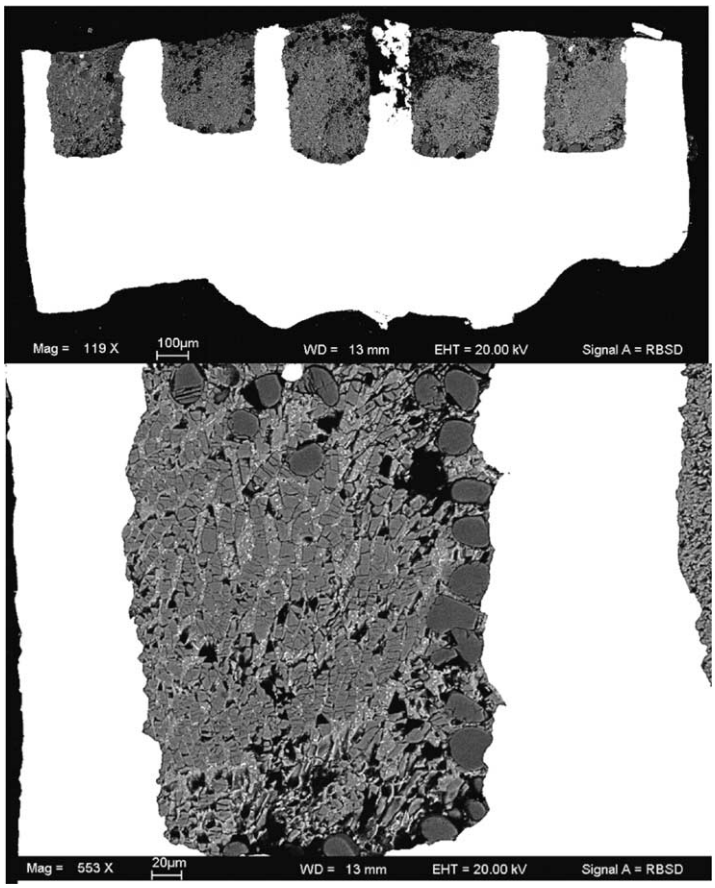

Fig. 5. A section through a 2 mm diameter multi-chamber Re sample capsule (top) containing five samples of Mg_2SiO_4 melted at 18 GPa and 2200 °C. The enlargement of the far left chamber (below) shows rounded crystals of periclase in a melt that has crystallised during quenching. Each chamber is 0.2 mm in diameter and contains an almost identical proportion of crystals and melt, which indicates very minor temperature differences between the chambers and therefore a low radial temperature gradient. The thermocouple was in contact with the bottom side of the capsule and the top section has been removed in order to determine the correct orientation for a cross-section exposing all chambers. Such capsules are used to determine relative melting temperatures of different compositions.

larger sample volume increases the precision of velocity determinations and allows better control over the sample environment such that sample deformation can be avoided. Larger volumes also benefit chemical diffusion experiments, particularly when diffusion is either rapid, such as in silicate melts, (e.g. Reid, 2003) or strongly temperature dependent.

Acknowledgements

We would like to express our thanks to G. Herrmannsdörfer, E. Ohtani, the firm of Voggenreiter (Mainleus), the firm of Paschhold (Hochstadt), M. Schmidt, H. Fischer, J. Peyronneau, Y. Xu, C. Holzapfel and J. Kung for help in the development and testing of the 5000 t multianvil system. The original manuscript was improved by the constructive comments of E. Ito and an anonymous reviewer. Funding was generously provided by the Free State of Bavaria.

References

Canil, D., 1994. Stability of clinopyroxene at pressure-temperature conditions of the transition zone. Phys. Earth Planet Int. 86, 25–34.

Dunn, K.J., Bundy, F.P., 1978. Materials and techniques for pressure calibration by resistance-jump transitions up to 500 kilobars. Rev. Sci. Instrum. 49, 365–370.

Fei, Y., Saxena, S.K., Navrotsky, A., 1990. Internally consistent thermodynamic data and equilibrium phase relations for compounds in the system MgO–SiO_2 at high pressure and high temperature. J. Geophys. Res. 95, 6915–6928.

Getting, I.C., 1998. New determination of the bismuth I-II equilibrium pressure: a proposed modification to the practical pressure scale. Metrologia 35, 119–132.

Kawai, N., Endo, S., 1970. The generation of ultrahigh hydrostatic pressures by a split sphere apparatus. Rev. Sci. Instrum. 41, 1178–1181.

Kawai, N., Togaya, M., Onodera, A., 1973. New device for pressure-vessels. Proc. Jpn. Acad. 8, 623–626.

Khedari, J., Benigni, P., Rogez, J., Mathieu, J.C., 1995. New apparatus for thermal diffusivity measurements of refractory solid materials by the periodic stationary method. Rev. Sci. Instrum. 66, 193–198.

Kohn, S.C., Brooker, R.A., Frost, D.J., Slesinger, A.E., Wood, B.J., 2002. Ordering of hydroxyl defects in hydrous wadsleyite (β-Mg_2SiO_4). Am. Miner. 87, 293–301.

Liebermann, R.C. and Wang, Y., 1992. Characterization of sample environment in a uniaxial split-sphere apparatus. In: Syono, Y., Manghnani, M.H. (Eds.), High-Pressure Research: Application to Earth and Planetary Sciences. AGU, Washington, DC, pp. 19–31.

Lloyd, E.C., 1971. Accurate characterization of the high pressure environment. NBS Special Publication No. 326, Washington DC, pp. 1–3.

Morishima, H., Kato, T., Suto, M., Ohtani, E., Urakawa, S., Utsumi, W., Shimomura, O., Kikegawa, T., 1994. The phase boundary between α and β-Mg_2SiO_4 determined by in situ X-ray observation. Science 265, 1202–1203.

Ohtani, E., Irifune, T., Hibberson, W.O., Ringwood, A.E., 1987. Modified split-sphere guide block for practical operation of a multiple-anvil apparatus. High Temp. High Pressures 19, 523–529.

Onodera, A., Ohtani, A., 1980. Fixed points for pressure calibration above 100 kbars related to semiconductor-metal transitions. J. Appl. Phys. 51 (5), 2581–2585.

Reid, J., 2003. Transport Properties of Silicate Liquids at High Pressure. PhD thesis, University of Bayreuth, 2003.

Rubie, D.C., 1999. Characterising the sample environment in multianvil high-pressure experiments. Phase Transitions 68, 431–451.

Susaki, J., Akaogi, M., Akimoto, S., Shimomura, O., 1985. Garnet-perovskite transformation in $CaGeO_3$: in-situ X-ray measurements using synchrotron radiation. Geophys. Res. Lett. 12, 729–732.

Suzuki, A., Ohtani, E., Morishima, H., Kubo, T., Kanbe, Y., Kondo, T., 2000. In situ determination of the phase boundary between wadsleyite and ringwoodite in Mg_2SiO_4. Geophys. Res. Lett. 27, 803–806.

Wade, J., Wood, B.J., 2002. A high-temperature (3000 K) assembly for piston cylinder experiments. Geochem. Geophys. Geosyst. 3, 1006.

Walter, M.J., Thibault, Y., Wei, K., Luth, R.W., 1995. Characterizing experimental pressure and temperature conditions in multianvil apparatus. Can. J. Phys. 73, 273–286.

Walker, D., Carpenter, M.A., Hitch, C.M., 1990. Some simplifications to multianvil devices for high pressure experiments. Am. Miner. 75, 1020–1028.

Xu, Y., Shankland, T.J., Rubie, D.C., Langenhorst, F., 2004. Thermal diffusivity measurements of olivine, wadsleyite and ringwoodite to 20 GPa and 1100 °C. Phys. Earth Planet Inter. doi: 10.1016/j.pepi.2004.03.005.

Yoneda, A., Yamamoto, S., Kato, M., Swamoto, H., Kumazawa, M., 1984. The use of composite metal gaskets to improve pressure generation in multiple anvil devices. High Temp. High Pressures 16, 637–656.

Zhang, J., Li, B., Utsumi, W., Liebermann, R.C., 1996. In situ X-ray observations of the coesite-stishovite transition: reversed phase boundary and kinetics. Phys. Chem. Miner. 23, 1–10.